LAWRENCE
LIVERMORE
NATIONAL
LABORATORY

UCRL-TR-227174

Notes on Longitudinal Dynamics in UMER

J.R. Harris

January 10, 2007

This work was performed under the auspices of the U.S. Department of Energy by University of California, Lawrence Livermore National Laboratory under Contract W-7405-Eng-48.

Notes on Longitudinal Dynamics in UMER.

John R. Harris

January 5, 2007

1. Beam Expansion.

Longitudinal expansion of the UMER beam is governed, to first order, by the one-dimensional cold fluid model (CFM) [1]. For an initially-rectangular beam, this model predicts erosion of the beam ends at a speed dependent on the "sound velocity,"

$$c_0 = \sqrt{\frac{qg\lambda_0}{4\pi\varepsilon_0 m\gamma^5}} \tag{1}$$

where q is the electron charge, λ_0 is the initial line charge density in the flat top, ε_0 is the permittivity of free space, m is the mass of the electron, γ is the relativistic factor, and $g = \alpha + 2\ln\left(\frac{b}{a}\right)$ is a geometry factor of order one where b is the beam pipe radius, a is the beam radius, and α is a constant to be discussed below. For comparison to experiment, the 20%-80% rise time at the beam ends, and the 20%-20% and 80%-80% beam lengths are useful. These are defined by the equations [2]

$$\tau_{80-20}(s) = \frac{3(0.447)c_0}{c^2\beta^2}s \tag{2}$$

$$\tau_{20-20}(s) = \tau_0 + \left|6\left(\sqrt{0.2} - \frac{2}{3}\right)\right|\frac{sc_0}{c^2\beta^2} \tag{3}$$

$$\tau_{80-80}(s) = \tau_0 - \left|6\left(\sqrt{0.8} - \frac{2}{3}\right)\right|\frac{sc_0}{c^2\beta^2}, \tag{4}$$

where s is the distance traveled by the beam, $c\beta$ is the beam velocity, and τ_0 is the initial length of the beam in seconds. These quantities are illustrated by Figure 1. Measurements were carried out on UMER to test the CFM [2]. The measured rise time at the head and 80%-80% beam length agreed well with the CFM and equations (2) and (4),

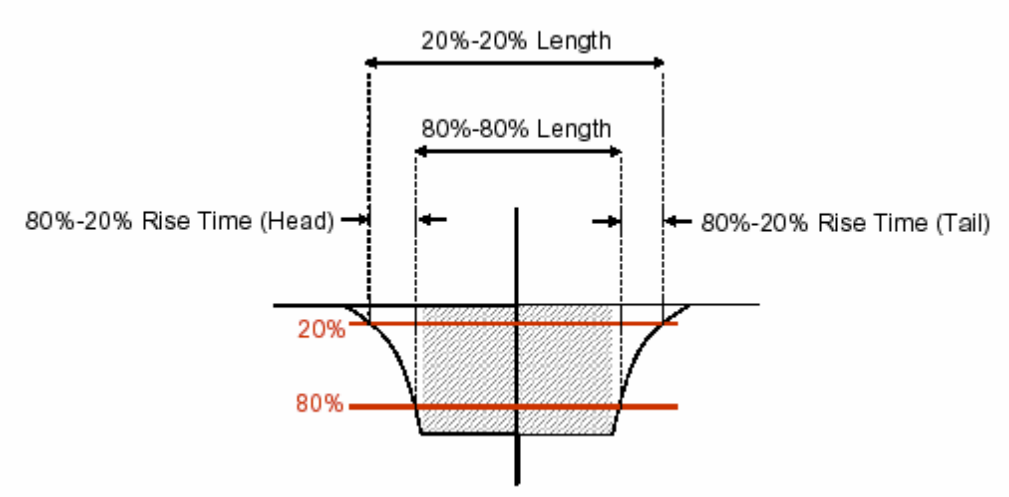

Figure 1: Illustration of 80%-20%, 80%-80%, and 20%-20% quantities [2].

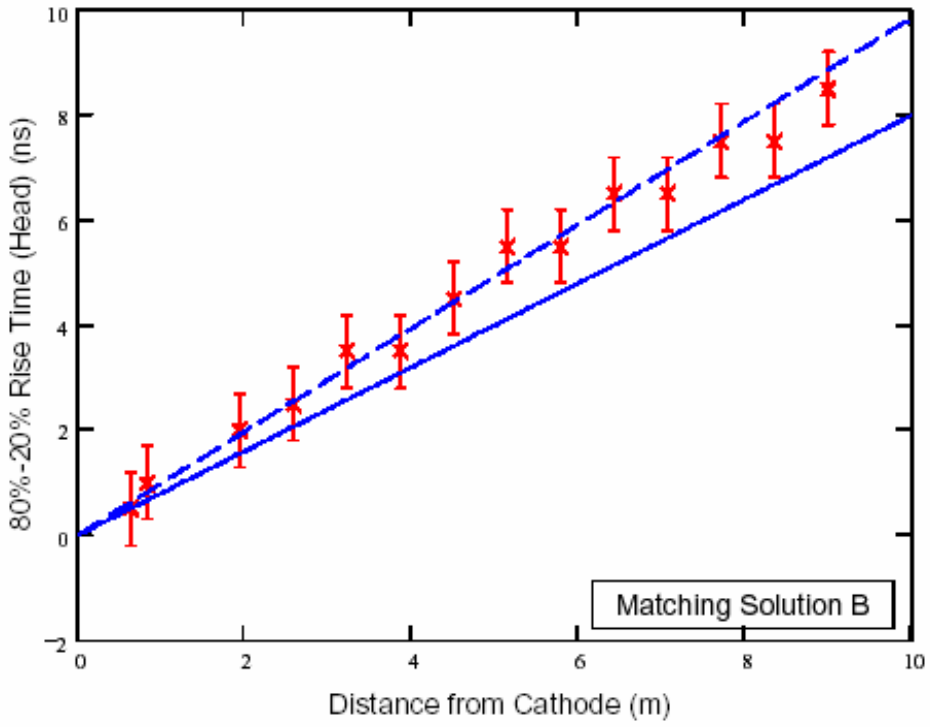

Figure 2. 80%-20% rise time for beam head, measured for a 100 mA beam in UMER, compared to theory for $\alpha = 0$ (solid), and $\alpha = 1$ (dash) [2].

as shown in Figures 2 and 3. However, the rise time at the tail and the 20%-20% beam length showed much poorer agreement with theory, as shown in Figures 4 and 5. This is believed to be caused by a transverse-longitudinal coupling due to the presence of a "bump" on the beam tail [2]. This bump (Fig. 6) is believed to be produced in the gun and due to irregularities on the cathode pulser waveform. By modifying this waveform, it may be possible to eliminate the bump and produce improved agreement with the CFM.

2. Optimum Beam Length in Absence of Longitudinal Focusing.

Despite this discrepancy, both the head and tail expansion *on average* appears to agree well with the CFM. In the UMER ring, the useful lifetime of the beam is governed by (1) the amount of time before the head and tail meet and the beam fills the entire ring, and (2) the amount of time before the beam flat top disappears. The full length of the beam as a function of distance traveled is

$$L = L_0 + \frac{4c_0 s}{c\beta}, \tag{5}$$

And the flat top length of the beam is given by

$$l = L_0 - \frac{2c_0 s}{c\beta}, \tag{6}$$

where $c\beta$ is the beam velocity, L_0 is the initial length of the beam, and s is the distance traveled. If the initial beam length is very short, then the flat top will erode completely before the beam expands to fill the ring, and the flat top length will be the limiting factor. If the initial beam length is very long, then the beam will expand to fill the ring before the flat top erodes, and the beam length will be the limiting factor. In the optimal case, both limiting factors will be reached simultaneously. These three cases are shown in Figure 7. In this case, eq. (5) gives

$$L_{0,OPT} = C - \frac{4c_0 s}{c\beta} \tag{7}$$

and eq. (6) gives

$$L_{0,OPT} = \frac{2c_0 s}{c\beta}, \tag{8}$$

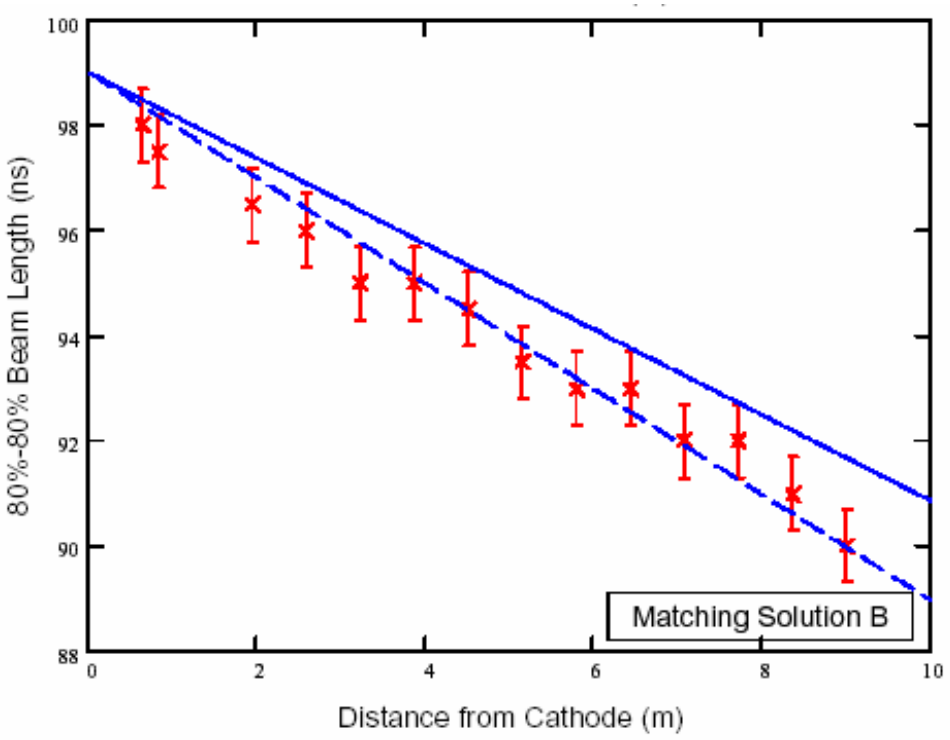

Figure 3. 80%-80% beam length, measured for a 100 mA beam in UMER, compared to theory for $\alpha = 0$ (solid), and $\alpha = 1$ (dash) [2].

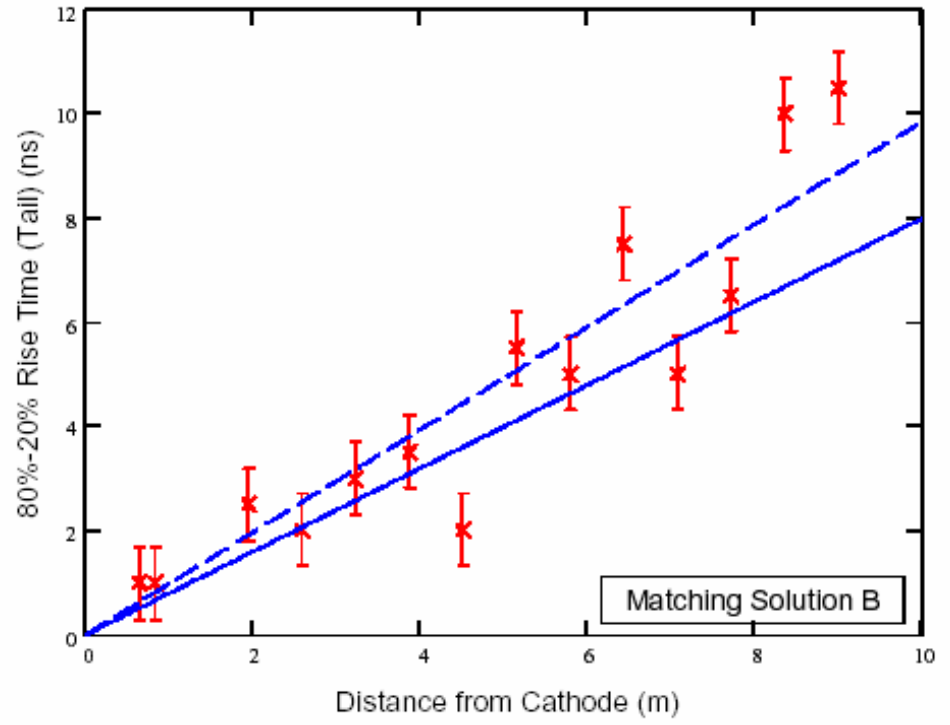

Figure 4. 80%-20% rise time for beam tail, measured for a 100 mA beam in UMER, compared to theory for $\alpha = 0$ (solid), and $\alpha = 1$ (dash) [2].

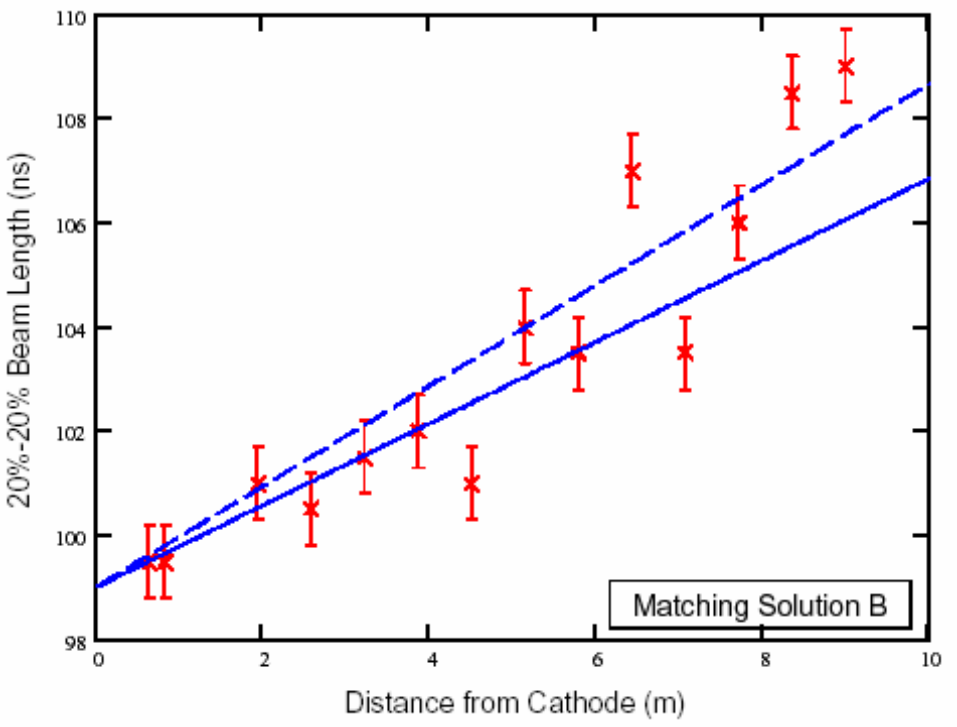

Figure 5. 20%-20% beam length, measured for a 100 mA beam in UMER, compared to theory for $\alpha = 0$ (solid), and $\alpha = 1$ (dash) [2].

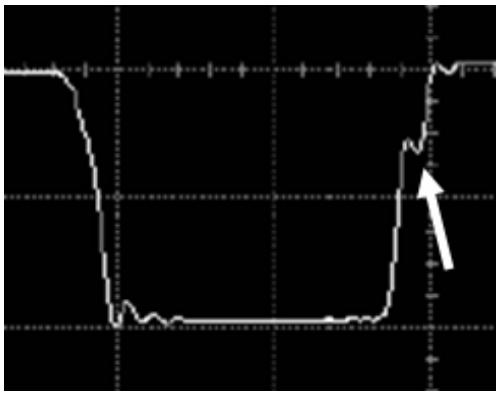

Figure 6. "Bump" observed on UMER beam pulse [2].

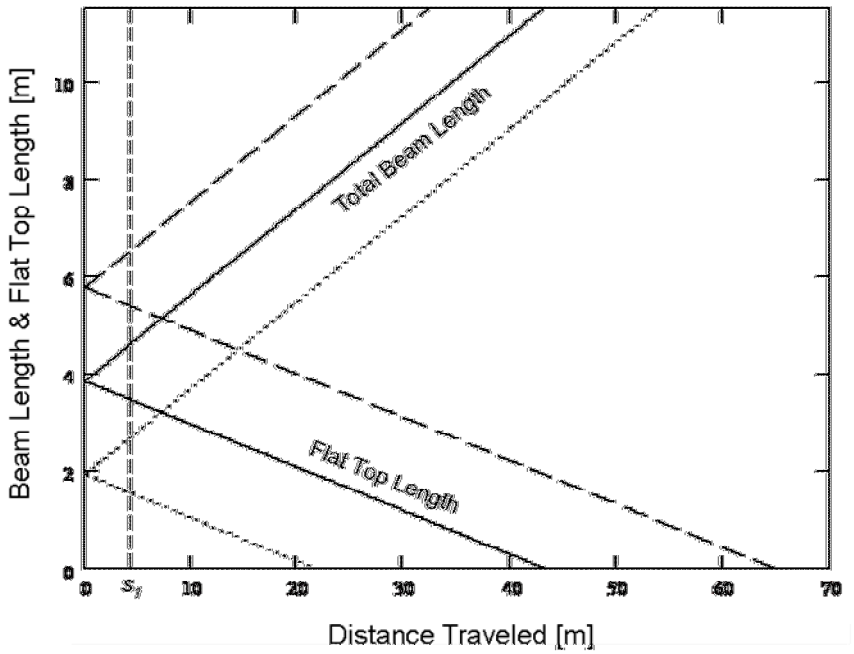

Figure 7. Total beam length and beam flat top length as a function of distance traveled in UMER for 100 mA beams with initial length of 1.92 m (dot), 3.84 m (solid), and 5.76 m (dash). A geometry factor of 3 and β of 0.2 are assumed.

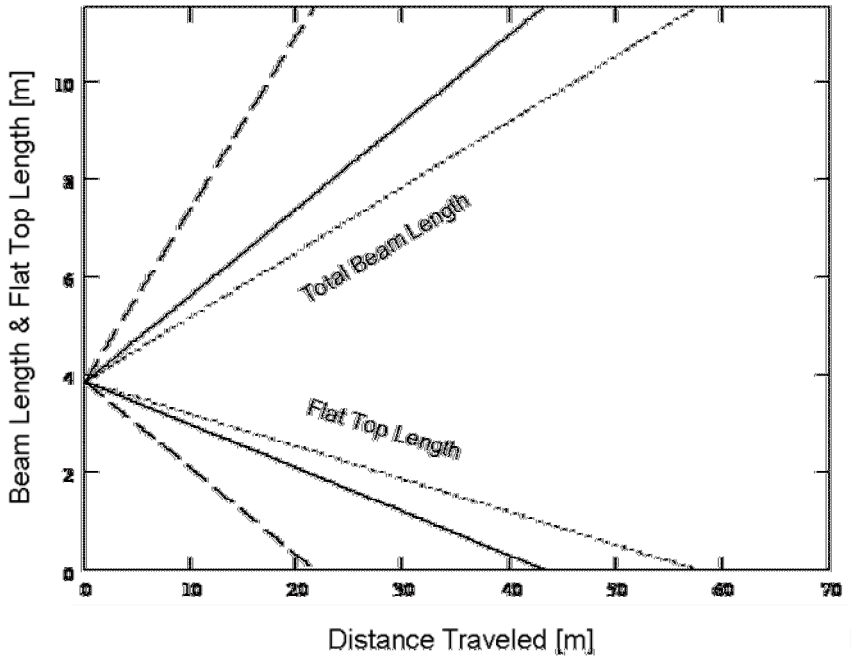

Figure 8. Total beam length and beam flat top length as a function of distance traveled in UMER for 100 mA beams with initial length of 3.84 m, for sound speeds of 2.00 Mm/s (dot), 2.67 Mm/s (solid), and 5.35 Mm/s (dash). A geometry factor of 3 and β of 0.2 are assumed.

so that the optimum beam length is

$$L_{0,OPT} = \frac{C}{3}, \tag{9}$$

where C is the UMER ring circumference. Expressed in seconds, the optimum beam length is

$$\tau_{0,OPT} = \frac{C}{3c\beta}. \tag{10}$$

Thus, the optimum initial length does not depend on beam current, although the useful lifetime of the beam does, as shown in Figure 8.

This analysis did not explicitly consider the expansion occurring as the beam travels through the injection section. However, this does not change the results, as it corresponds to a simple translation of the origin from $s = 0$ to $s = s_1$ as shown in Figure 7.

3. Significance of α.

The geometry factor arises in the derivation of the longitudinal electric field [3], and the value of α depends on assumptions made regarding the beam geometry and density. If the volume charge density is assumed to be uniform everywhere, then changes in line charge density are due to changes in beam radius, and $\alpha = 0$. If the beam radius is assumed to be uniform everywhere, then changes in line charge density are due to changes in volume charge density, and α varies from $\alpha = 0$ at the beam edge to $\alpha = 1$ on the beam axis. The former case is generally assumed for space charge dominated beams, and the latter case is generally assumed for emittance dominated beams [4].

In principle, the value of α gives useful information regarding the distribution of charge in the beam. It relates to the energy stored in the beam, and may be expected to change as the beam evolves [2]. However, this information is difficult to access experimentally, for several reasons. First, the beam pipe radius is a well-defined value, while the beam radius is less well-defined. The choice of beam radius measurement (FWHM, RMS, etc.) will therefore change the ratio $\frac{b}{a}$, and therefore will change the

measured value of α. In some cases, the difference resulting between a change from $\alpha = 0$ to $\alpha = 1$ is smaller than the experimental error. The beam in general will not be on-axis and cylindrically symmetric as assumed in the derivation of the electric field, and it is not clear how this will affect α. Finally, the radius changes along the beam and during the beam's life due to current variations and periodic focusing. These and other issues make the meaning of α unclear.

4. Longitudinal Focusing.

Longitudinal focusing is possible because of the time-reversibility of the CFM equations [5]. Induction gap design, as well as focusing voltages and waveforms for rectangular and parabolic pulses have been discussed in detail elsewhere [5-13]. Note that the method described in [5], where the beam flat top is allowed to erode fully before longitudinal focusing is applied is problematic because the dynamics become nonlinear at this point, and therefore emittance and entropy growth may occur and lead to irreversibility. This may cause the beam pulse shape to degrade. A better method is to apply longitudinal focusing long before the flat top has fully eroded.

In the standard longitudinal focusing lattice arrangement for UMER, three induction gaps are located at RC1, RC7, and RC13. This scheme accomplishes the first-order longitudinal focusing lattice requirement, that the total distance between adjacent induction gaps must be equal, and that the distance between adjacent induction gaps is twice the distance between the cathode and the first induction gap [12, 14, 15]. This requirement causes the beam length to be identical at each induction gap, and therefore allows all induction gaps to use the same longitudinal focusing waveform. However, the location of an induction gap at RC1 is problematic because of the need to have a BPM there to ensure a correct beam trajectory for matching into the ring [16]. The first-order requirements may also be satisfied by locating a single induction gap at RC7 [15]. Note that reducing the number of induction gaps does not increase the peak voltage needed (which is set by the sound speed, and therefore the beam current and energy, not the distance traveled). However, the end regions in the beam will be larger, and therefore the longitudinal focusing pulser requirements will change somewhat. They will be simplified

because the rise time of the "ear fields" will be reduced, but complicated by the need for a core with a larger volt-second product. Also, note that the induction gap does not have to be used on each passing of the beam; rather it may be used only every 2,3,...n turns. This may also relax some of the longitudinal focusing requirements, provided that the beam does not fill the ring and the flat top is not lost. Note that simulations done by Yun Li indicate increased loss of beam particles due to the use of three induction gaps, as compared with the use of no induction gaps [17]. Presumably the use of only one induction gap will also be better than three from this perspective. In addition, ref. [10] indicates that reducing the number of induction gaps will reduce the growth of energy spread and beam breakup effects.

References

[1] A. Faltens, E.P. Lee, and S.S. Rosenblum, J. Appl. Phys. **61**, p. 5219 (1987).

[2] J.R. Harris, Doctoral Dissertation, University of Maryland (2005). Online: http://hdl.handle.net/1903/2906

[3] M. Reiser, *Theory and Design of Charged Particle Beams*, Wiley: New York (1994).

[4] I. Haber, personal communication.

[5] D.X. Wang, Doctoral Dissertation, University of Maryland (1993).

[6] J. Deng, UMER Technical Note UMER-021097-JD (E-Ring-97-04) (1996).

[7] M. Reiser, UMER Technical Note UMER-041996-MR (E-Ring-96-08) (1996).

[8] J. Deng, UMER Technical Note UMER-042696-JD (E-Ring-96-04) (1996).

[9] J.G. Wang, UMER Technical Note UMER-042696-JGW (E-Ring-96-11) (1996).

[10] J. Deng, UMER Technical Note UMER-051096-JG (E-Ring-96-14) (1996).

[11] Y. Li, UMER Technical Note UMER-100397-YL (E-Ring-97-41) (1997).

[12] Y. Li, UMER Technical Note UMER-071599-YL (UMER 99 YL) (1999).

[13] J.R. Harris, Master's Thesis, University of Maryland (2002). Online: http://www.umer.umd.edu/publications/Theses/

[14] J. Deng, UMER Technical Note UMER-100496-JD (E-Ring-96-42) (1996).

[15] J.R. Harris, "Modifications to Longitudinal Focusing System in UMER," (2004).

[16] R. Kishek, personal communication.

[17] Y. Li, UMER Technical Note UMER-071798-YL (E-Ring-98-27) (1998).